COMPARING ATMOSPHERIC CORRECTION METHODS FOR LANDSAT OLI DATA

Esthi Kurnia Dewi*⁾ and Bambang Trisakti
Remote Sensing Application Center, LAPAN
*⁾E-mail: esthikd@gmail.com

Abstract. Landsat data used for monitoring activities to land cover because it has spatial resolution and high temporal. To monitor land cover changes in an area, atmospheric correction is needed to be performed in order to obtain data with precise digital value picturing current condition. This study compared atmospheric correction methods namely Quick Atmospheric Correction (QUAC), Dark Object Subtraction (DOS) and Fast Line-of-sight Atmospheric Analysis of Spectral Hypercubes (FLAASH). The correction results then were compared to Surface Reflectance (SR) imagery data obtained from the United States Geological Survey (USGS) satelite. The three atmospheric correction methods were applied to Landsat OLI data path/row126/62 for 3 particular dates. Then, sample on vegetation, soil and bodies of water (waterbody) were retrieved from the image. Atmospheric correction results were visually observed and compared with SR sample on the absolute value, object spectral patterns, as well as location and time consistency. Visual observation indicates that there was a contrast change on images that had been corrected by using FLAASH method compared to SR, which mean that the atmospheric correction method was quite effective. Analysis on the object spectral pattern, soil, vegetation and waterbody of images corrected by using FLAASH method showed that it was not good enough eventhough the reflectant value differed greatly to SR image. This might be caused by certain variables of aerosol and atmospheric models used in Indonesia. QUAC and DOS made more appropriate spectral pattern of vegetation and water body than spectral library. In terms of average value and deviation difference, spectral patterns of soil corrected by using DOS was more compatible than QUAC.

Keywords: *Landsat, atmospheric correction, QUAC, FLAASH, DOS, surface reflectance*

1   INTRODUCTION

Over the last decades, Indonesia has experienced significant changes on its land cover due to illegal logging and land opening, as well as peat land combustion. Remote sensing data were widely used for land cover monitoring activities. They were Ginting et al. (2012) who conducted research on land cover by utilizing remote sensing data, particularly Landsat data to monitor in Karo Regency; and Yulius et al. (2014) who monitored land cover changes on Bungus Teluk Kabung Bay. Furthermore, Tampubolon *et al.*, (2015) analyzed the changes on critical land of Medan; Tuni et al. (2013) classified land closure or land used in North Halmahera; and Ceccarelli et al. (2013) who examined land cover in Oristano and Campania, Provinces of Rome.

However, Landsat imagery data that had been recorded by Indonesian Aeronautics and Space Agency (LAPAN) could not be used directly to extract land cover information, since the data contained noise caused by atmospheric effects. Atmospheric noises that might afffect the quality of remote sensing imagery were molecules and aerosols scattering, water vapor absorbtion, carbon

dioxide, oxygen, ozone, as well as light effect and transmittance on the atmosphere (Zhang *et al.*, 2010).

To eliminate noise which might cause image distortion, sun correction and atmospheric correction needed to be done. In relation to position of the sun. Sun correction was performed by converting digital number (DN) to reflectance value. Then Atmospheric correction was done to reduce or eliminate atmospheric effect and to obtain reflectant value on the suface. Some atmospheric correction methods were, for example, digital number (DN) used directly for transformation reflection by Smith et al (1999), Dark Object Subtraction (DOS) by (Zhang et al., 2010; Trisakti et al., 2014), Fast Line-of-sight Atmospheric Analysis of Spectral Hypercubes (FLAASH), as well as Quick Atmospheric Correction (QUAC), 6S, and ATCOR 2-3.

This research utilized atmospheric correction method which compatible with data quality, data availability, and research purposes. Some previous studies on the correction method had been performed. Such as Somdatta et al. (2011) who implemented both FLAASH and QUACC methods on hyperion data. They conclude FLAASH was better than QUAC in terms of atmospheric correction result. Guo *et al.* (2012) who studied the spot data with both methods found that FLAASH was more effective to reduce noise than QUAC. Furthermore, Nazeer *et al.* (2001) who implemented 6S, FLAASH, ATCOR, DOS, and ELM methods on Landsat 7 Data and compared the results with Surface Reflectance (SR) data from USGS, found that DOS and 6S generated the most appropriate and consistent result. Cui et al. (2001) also conducted a study on Landsat TM 1, Landsat TM 2, Landsat TM 3, Landsat TM 4, Landsat TM 5, and Landsat TM 7 with DOS, DOSCOST, DOS-Constant, and DOS-Iteration. At last, Cui et al choose DOS as the best model to acquire quantitative and

historical data, and suggest DOS-Iteration since the method gathered broader spectral range. Lee et al. (2000) who examined Landsat 5 Data with FLAASH, Foster and 6S models found that FLAASH was the best model. Nguyen et al (2015) who reviewed QUAC, FLAASH and 6S models with Landsat 5 Data stated that 6S was the best model which resembled on ground condition. Afterall, this research aimed to analyze a suitable atmospheric correction model for Landsat OLI data in order to retrieve Indonesian land cover information which corresponded to actual coverage.

To achieve the above result, an analysis was performed on some atmospheric correction methods, i.e. FLAASH, QUAC and DOS for Landsat OLI path/row 126/62 in certain area of study compared to USGS's Surface Reflectance data which had corrected. This research was aimed to find the most accurate and consistent method in accordance with actual condition.

2. MATERIALS AND METHODOLOGY
2.1 Data

Remote sensing data used in this study were Landsat 8 level LT1 which was recorded by LAPAN Remote Sensing Center, Parepare and Rumpin with 3 different dates and Surface Reflectance data from USGS as the comparative data (Table 2-1).

Table 2-1: Satelite images used in this research

Number	Data Acquisition	Explanation	Path/Row
1	June 21, 2014	Landsat 8	126/62
2	July 26, 2015	Landsat 8	126/62
3	May 9, 2016	Landsat 8	126/62
4	July 26, 2015	USGS *Surface Reflectance*	126/62

For spectral analysis purpose, sampling process was carried out on

vegetation (forests), water and soil. The data used were acquired in May, June, July or during dry season with 1 to 7 spectral bands. The spectral bands were choosen since they were often used in classifying land cover. The area analyzed was Lake Kerinci surroundings, which included the lake itself, sea, agricultural lands, and soil.

Sample observed in this study were vegetation (forest), body of water and soil, each was selected from three sample locations (Figure 2-1). Sample taken were then compared to Surface Reflectance data. Reference value of Landsat OLI spectral for vegetation, water and settlement were shown on Figure 2-2 below.
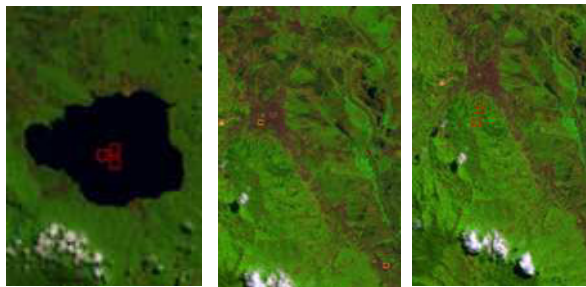
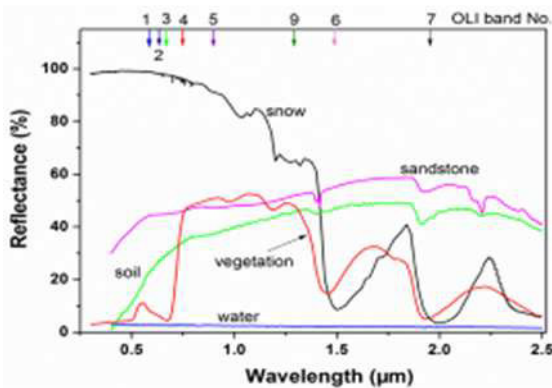Figure 2-1: Sampling on water (a), soil (b), vegetation (c) on Landsat imagery

Figure 2-2: Landsat 8 object profile of water, soil and vegetation Source: Journal Optics Express, 2014

2.2 Methods
2.2.1 FLAASH Model

FLAASH was an atmospheric correction tool to fix visible band, NIR, SWIR. This model eliminated air and light influences, as well as removed interference due to reflectivity parameter, emissivity, surface temperature and physical surface reflection.

FLAASH began with a standard equation of spectral glow from single pixel received by standard Lambertian planar (the closest Lambertian planar), which was accepted by a sensor based on solar spectrum (excluding thermal radiation), with the following formula:

$$L' = \left(\frac{A\rho}{1-\rho_e S}\right) + \left(\frac{B\rho_e}{1-\rho_e S}\right) + L_a \qquad (2\text{-}1)$$

L was the light for single pixel received by sensor; ρ was pixel surface reflectance; ρ_e was average surface reflectance for the pixel and its surrounding; S was the accumulation of sunlight reflection and diffusion by atmospheric particles; L_a was the radiance when atmospheric radiation penetrated sensor. A and B were coefficient determined by atmospheric and geometric conditions of the underlying surface but had nothing to do with surface reflectance. ($A\rho$ / ($1-\rho_e$ S)) represented radiation energy which penetrated directly into the sensor from the target's surface, which indicated two cases: reflection occurs when the sun illuminates target surface; or the surrounding surface reflected through the atmosphere and shined in the target surface target before another reflection. ($B\rho_e$ / ($1-\rho_e$ S)) showed total radiation that went into sensor from the surface through the atmosphere. ρ and ρ_e explained "proximity effect" of mixed pixel near the radiation caused by atmospheric scattering, with the assumption $\rho = \rho e$. However, significant error might occur due to fog or strong contrast on the surfaces.

According to Equation 1, surface reflection could be calculated pixel by pixel. FLAASH used average radian spatial, ignoring "proximity effect", to get estimate equation (2) and to predict spatial reflectance. While, L_e was the average radiant image generated from imagery radian and spatial function.

$$L_e \approx \left(\frac{(A+B)\rho_e}{1 - \rho_e S} \right) + L_e \qquad (2\text{-}2)$$

Most of the atmospheric correction parameters used in this experiment were metadata of Landsat image, and specific parameter data as shown in Table 2-2. After getting the required parameters, the actual surface reflectance of all imageries were calculated using Equation 1 and Equation 2.

2.2.2 QUAC Model

QUAC was an atmospheric correction method for hyperspectral and multispectral of visible band, NIR and SWIR. QUAC initial principles differed from usual atmospheric correction method, because this approach was based on the values of light which penetrated the scene. QUAC was known as an empirical approach based on recording. This determined kinds of parameter received from the atmosphere directly during the recording, without additional information.

$$\rho' = (\rho_1 + \rho_2 + \cdots + \rho_n)/n \qquad (2\text{-}3)$$

The above equation showed QUAC model based on the experience of gathering average reflectance from diverse content such as spectrum of each section, n indicated the amount of spectrum

detected with shadows or cloud free basic scene. It mean that this correction would run faster. Below was QUAC Model flowchart (Figure 2-3).
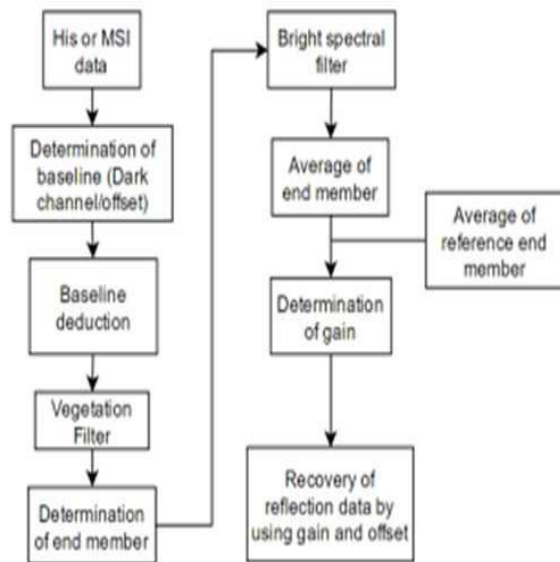

Figure 2-3: QUAC Model Flowchart
Source: ITT Visual Information Solutions (ITT VIS), "ENVI User's Guide, Version 4.8"

QUAC also utilized the sun elevation angle and central wavelength. If the sensor did not have precise radiation or wavelength, or the intensity of sunlight was unknown, corrections could still be performed by using this method within allowed scope of accuracy.

Table 2-2: Paramater used in FLAASH atmospheric correction

Data	Imagery Time	Sensor	Height of Sensor	Atmosphere Model	Sun Elevation	Ground Elevation	Visibility
June, 21 2014	03:23:43	Landsat 8 OLI	705 km	Tropical	52.23908383	0.78 km	40 km
July, 26 2015	03:23:36	Landsat 8 OLI	705 km	Tropical	53.70803343	0.78 km	40 km
May, 9 2016	03:23:34	Landsat 8 OLI	705 km	Tropical	56.82897852	0.78 km	40 km

2.2.3 DOS Model

DOS was an image-based atmospheric correction. Chavez (1996) stated a basic assumption that few pixels radiances on covered by cloud image could be accepted by the satellite due to atmospheric scattering (path radiance). Considering the fact that there was very few target on the Earth surface was absolute black, it was assumed that one percent of minimum reflektansi was better than zero percent.

Landsat 8 data which was radiometrically corrected including ToA Reflectance dan sunlight correction. ToA Reflectance was corrected by converting the DN value to reflectance value. Based on USGS (2014), ToA Reflectance equation was:

$$\rho\lambda' = M\rho Qcal + A\rho \qquad (2\text{-}4)$$

Which:
$\rho\lambda'$ =ToA Reflectance, without correction of sunlight angle.
$M\rho$ =REFLECTANCE_MULT_BAND_x, in which x is Band number
$A\rho$ =REFLECTANCE_ADD_BAND_x, in which x is Band number
Qcal=Digital Number (DN) value

Then, image correction was conducted due to sunlight angle change, to eliminate DN value difference, with the following equation:

$$\rho\lambda = \rho\lambda'/(\cos(\theta SZ)) = \rho\lambda'/(\sin(\theta SE)) \qquad (2\text{-}5)$$

Which:
$\rho\lambda$ =ToA Reflectance
SE =sun elevation
SZ =zenith angle of the sun, where SZ = 90 ° - SE

After the sun elevation was approved, then correction was also performed on dark pixel. DOS assumes horizontal atmosphere on similar images needed a black target by substracting dark gray object pixel from grey value of each pixel on the image.

$$L_p = L_{\min} + L_{D01\%} \qquad (2\text{-}6)$$

Which:
$L_{\min}$ =the light that corresponded to digital value which was the total of all pixel which digital sum was lower or min DN value.
$L_{D01\%}$ =radiance of dark object which was assumed to have 0.01 reflectance value

To calculate Landsat Imagery

$$L_{min} = M_L * DN_{min} + A_L \qquad (2\text{-}7)$$

To calculate Object Radiance

$$L_{D01\%} = 0.01 * [(ESUN_\lambda * cos\theta_s * T_z) + E_{down}] * T_v / (\pi * d^2) \qquad (2\text{-}8)$$

So to calculate path radiance of the dark object

$$L_p = M_L * DN_{min} + A_L - 0.01 * [(ESUN_\lambda * cos\theta_s * T_z) + E_{down}] * T_v / (\pi * d^2) \qquad (2\text{-}9)$$

Assumed that
T_v =1
T_z =1
E_{down} =0

Untuk mencari ESUN Landsat 8 OLI adalah sebagai berikut

$$ESUN = (\pi * d^2) * \frac{Radiance\_Maximum}{Reflectance\_Maximum} \qquad (2\text{-}10)$$

Analysis stages of three atmospheric correction models (FLAASH, QUAC and DOS) compared to Surface Reflectance

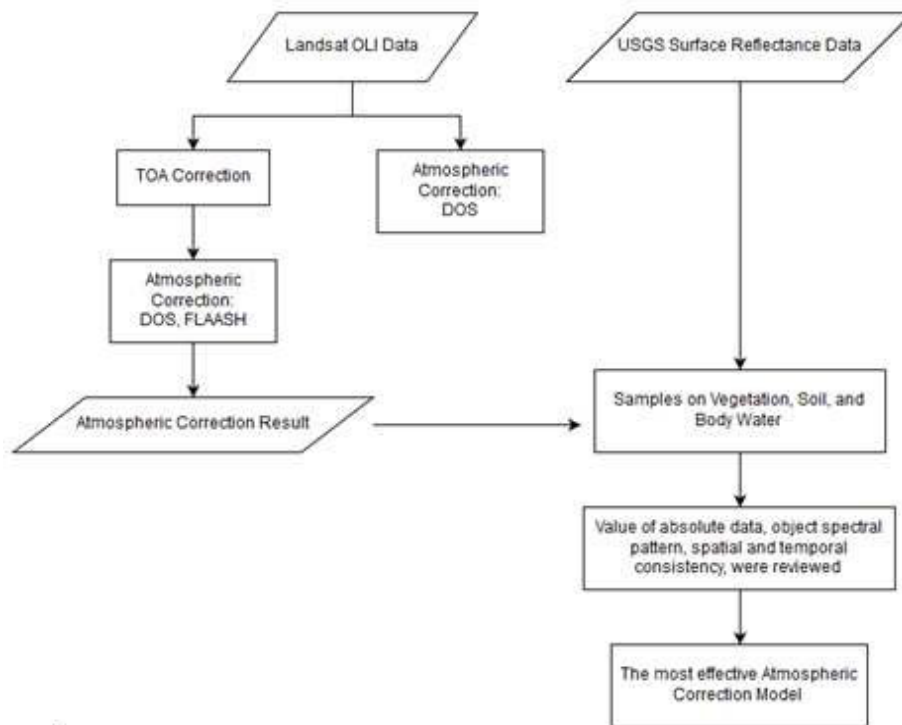data from the USGS were as follow (Figure 2-4).

Figure 2-4: Step To Compare Atmospheric Correction

3   RESULTS AND DISCUSSION

To analyze and compare the results of FLAASH, QUAC, and DOS atmospheric correction models with SR on Landsat 8 imagery data, it took visual review on the models after and before the correction, as well the reflectance feature of surface spectral curve.

3.1 Visual Contras Analysis Before and After Correction

Figure 3-1, 3-2 and 3-3 a, b, c, d are Landsat imageries with 3 different dates before and after FLAASH, QUAC, and DOS atmospheric correction with 6, 5, and 2 RGB bands combinations. Figure 3-4 was the Surface Reflectance of the USGS imagery in combination with 6, 5, and 2 RGB Bands. Visible changes were seen on the image, before and after correction. Before corrected, the image was darker due to the presence of atmospheric effects that reduced the image's contrast ratio of light and dark. After correction, imagery data got brighter and clearer. The quality of image was improved due to better

contrast ratio, which showed that the atmospheric correction was quite effective. These results were in accordance with previous research performed by Rahayu et al. (2001), which found brighter visual effect.

When the results of atmospheric correction were visually compared, FLAASH image had the highest contrast ratio. This fitted to Bong et al (2015) research finding that FLAASH model visually showed sharp contrast ratio compared to QUAC model.

Surface Reflectance (SR) of USGS was utilized as comparative model, since it best represented on field condition. In term of contrast ratio, image that was corrected with FLAASH model had the most similarity to SR. However, visual judgment only could not decide clearly whether FLAASH was the best model to represent the real condition. Thus, it took deeper analysis on spectral reflectance

curve by testing the quality of images on
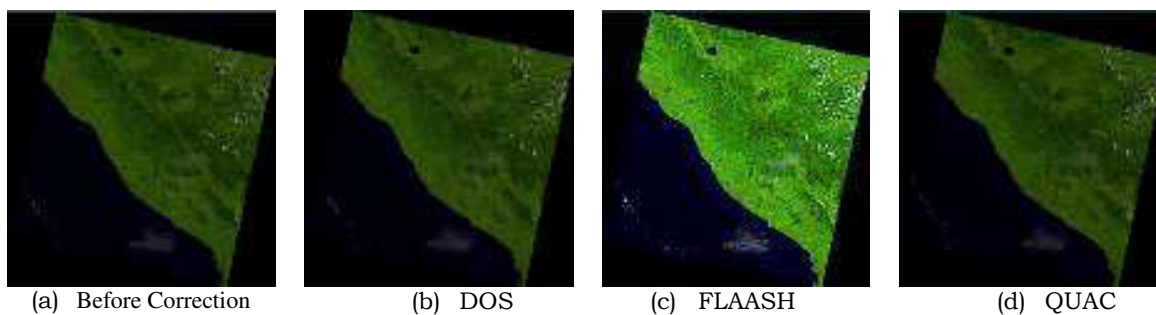each sample, region, and period of time.

| (a) Before Correction | (b) DOS | (c) FLAASH | (d) QUAC |

Figure 3-1: Visual analysis on Landsat 8 image acquired on June 21, 2014

| (a) Before Correction | (b) DOS | (c) FLAASH | (d) QUAC |
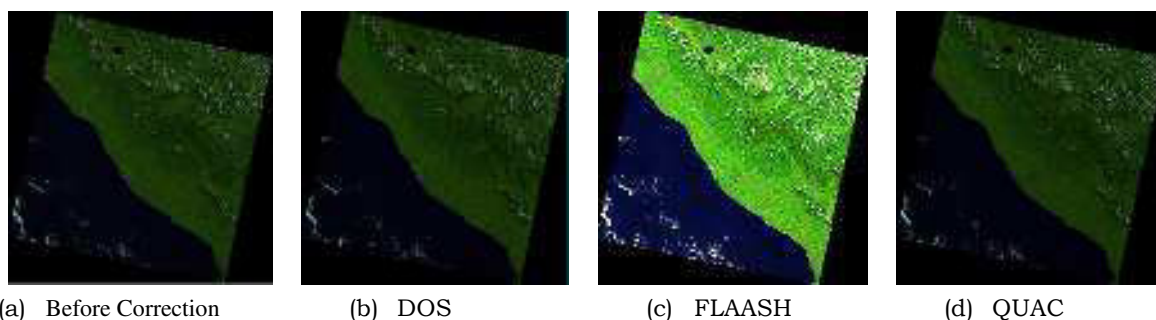
Figure 3-2: Visual Analysis on Landsat 8 Image Acquired on July 26, 2015

| (a) Before Correction | (b) DOS | (c) FLAASH | (d) QUAC |
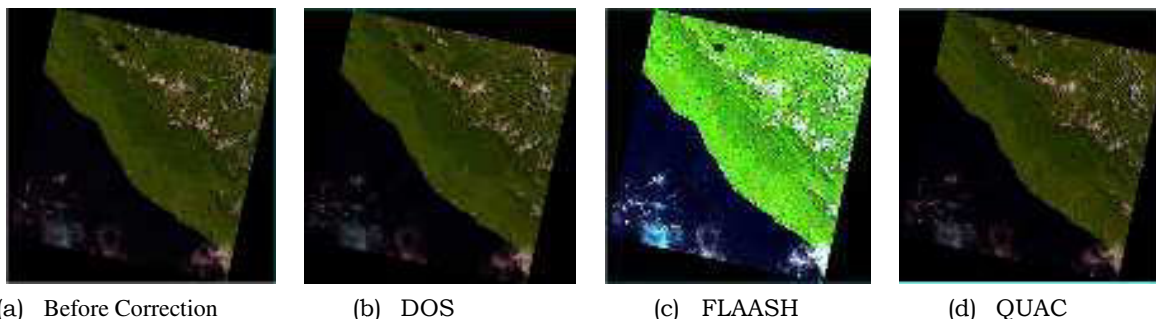
Figure 3-3: Visual Analysis on Landsat 8 Image Acquired on May 9, 2016

Figure 3-4: Visual Analysis on *Surface Reflectance* Image Acquired on July 26, 2015

3.2 Analysis Based on Spectral Reflectance Curve

Further analysis was conducted by observing the spectral pattern based on sampling test. Spectral results among samples with spectral consistency between regions and time, was observed.

3.2.1 Spectral curve between sampling

The spectral pattern of water body samples corrected by using FLAASH, QUAC and DOS models were compared with SR image. It was seen that QUAC and DOS images had almost similar pattern with SR image, while FLAASH had higher reflectance value (Figure 3-5).

When the spectral curve of the three corrected images were compared in terms of average difference to SR model, DOS model had the most nearly similar value of 0.002, followed by QUAC with 0.004 difference value, and FLAASH was the least similar with 0.05 difference value. In terms of data diversity, then image with the least deviation difference value against SR was DOS of 0.001, and followed by QUAC of 0.0029. Then FLAASH had the highest diversity of 0.053 (Figure 3-6). Spectral pattern of soil sample images corrected using FLAASH, QUAC and DOS models were compared with SR image. It showed that DOS image had almost the same spectral pattern with SR image, followed by QUAC and FLAASH with higher reflectance value (Figure 3-7).

In terms of average difference against SR model, it was concluded that the most approaching model was DOS with difference value of 0.009, followed by QUAC with 0.06 and FLAASH with 0.18. In terms of data diversity, then deviation difference of DOS model against SR was the most similar with 0.0027, followed by FLAASH with 0.034. QUAC had the highest diversity of 0.076 (Figure 3-8).

For vegetation (forest) sampling, spectral pattern of images corrected using FLAASH, QUAC and DOS models were compared to SR. It showed that DOS had almost the same spectral pattern to SR, followed by QUAC. FLAASH image had the highest reflectance value (Figure 3-9).

When average difference value was subtracted from the above models, it could be concluded that DOS was the most approaching model by 0.0049 difference, then QUAC by 0.043, and FLAASH by 0.128. As data diversity was reviewed, then DOS had the least deviation difference against SR by 0.0035, followed by QUAC of 0.053. FLAASH had the highest diversity of 0.123 (Figure 3-10).

The results of this study was in accordance with the research result of Nazer et al (2014), which stated that DOS and 6S had the most appropriate and consistent value with SR compared to FLAASH and QUAC models.
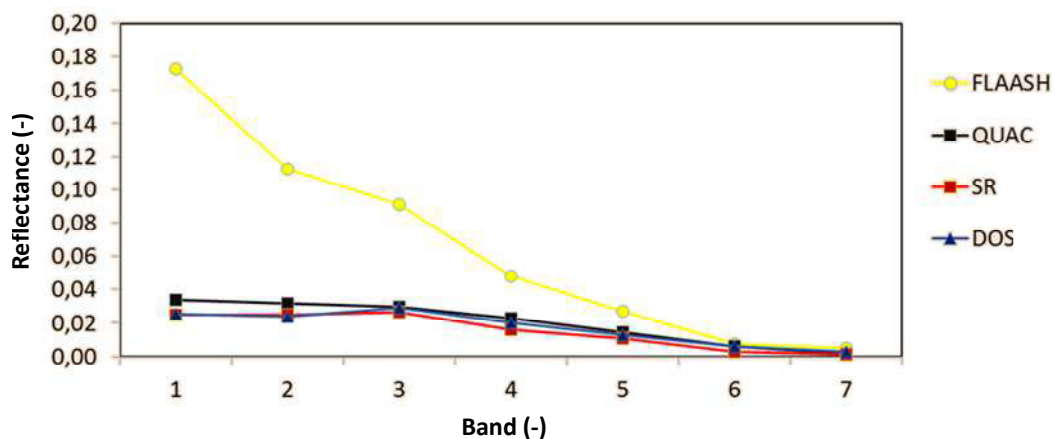

Figure 3-5: Visual Analysis of Surface Reflectance of Water in Image July 16, 2015
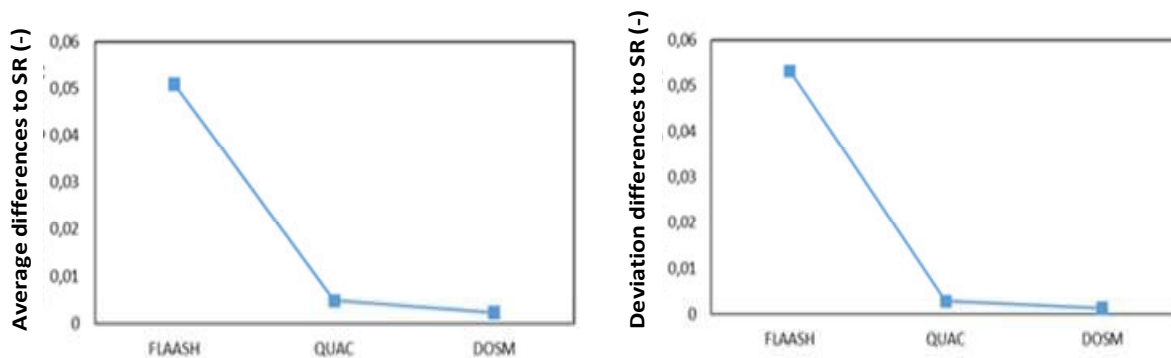
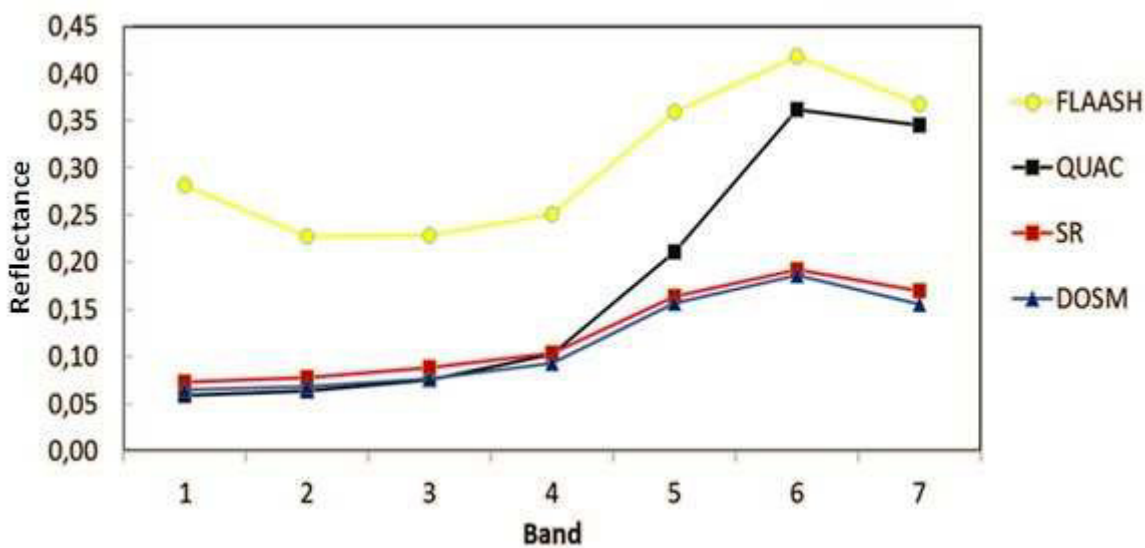Figure 3-6: Average and Deviation Difference of Water against SR

Figure 3-7: Visual Analysis of Surface Reflectance of Soil in Image July 16, 2015
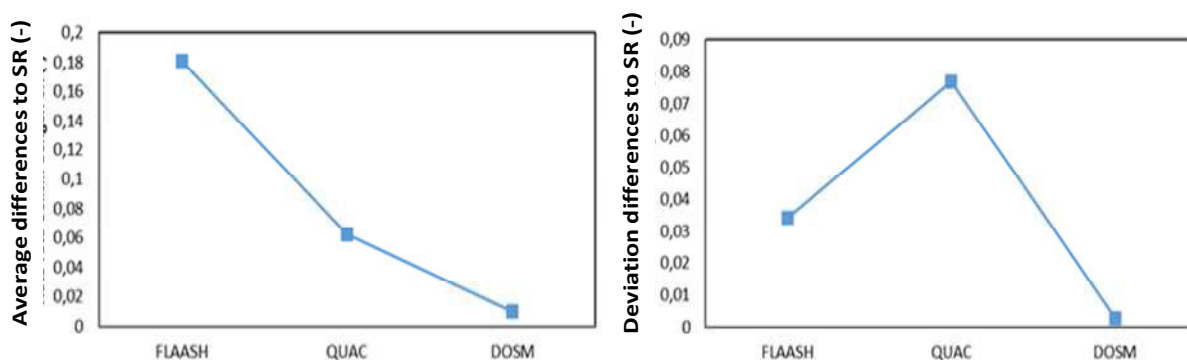

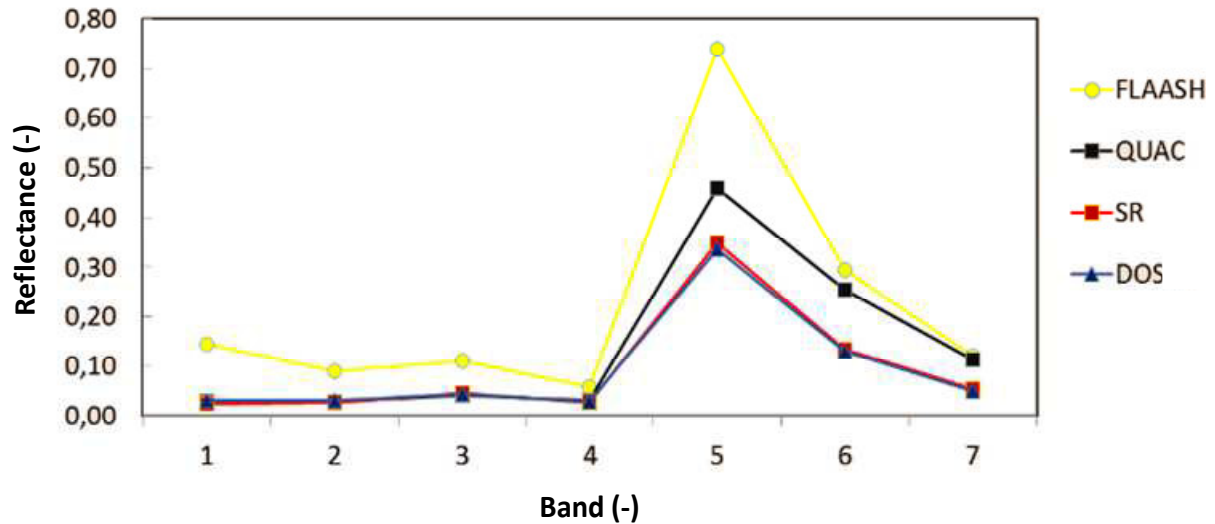Figure 3-8: Average and Deviation Difference of Soil against SR

Figure 3-9: Visual Analysis of Surface Reflectance of Vegetation in Image on July 26, 2015
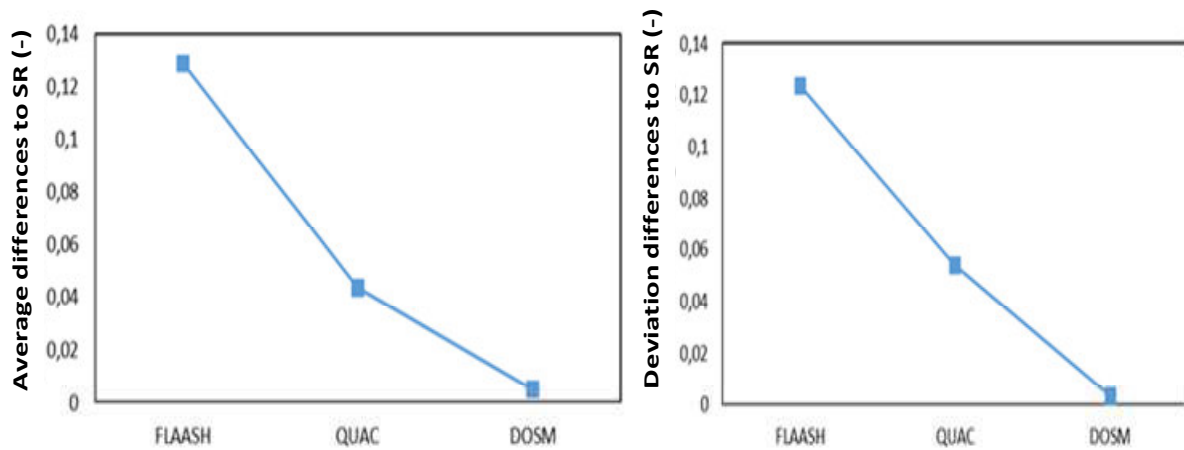

Figure 3-10: Average and Deviation Value of Vegetation against SR

3.2.2 Spatial spectral curve

Analysis on water sampling indicated that QUAC, SR, and DOS had almost similar average value. It mean that all samples were taken from similar location (Figure 3-11). As it is observed, water spectral profile taken from 3 different locations were almost identical to SR, which mean that the samples were taken correctly and consistently. FLAASH image also had similar and consistent pattern, but there was a difference in absolute value of visible band.

Spatial analysis on settlement or soil sampling showed that SR and DOS had almost the same average rating; which mean that samples were retrieved from the same location. QUAC and SR had similar visible bands, however absolute band value of NIR and SWIR change. FLAASH had almost the same pattern to SR, but higher absolute value (Figure 3-12). When it was reviewed, the spectral profile of settlement or soil taken from 3 different locations had almost similar value with SR (Figure 3-13), which mean that samples were taken correctly and consistently (Figure 3-14).

Spatial analysis on vegetation (forests) sampling indicated that SR and DOS had almost the same average rating. It mean that the samples were retrieved from similar location. In terms of band visible QUAC was similar to SR, but absolute value on NIR and SWIR bands changed. FLAASH had almost the same

pattern, but higher absolute value (Figure 3-15). Meanwhile, when spectral profile of vegetation (forest) in 3 different sample locations were reviewed, all had almost identical value to SR; which mean that sampling locations were correct and consistent (Figure 3-16).

Inter (spatial) location observation here was different to research conducted by Bongetal (2015) which found that FLAASH might generate better results than QUAC. This might happen since the type of aerosol variable and atmospheric conditions used in Indonesia differed in previous research areas.
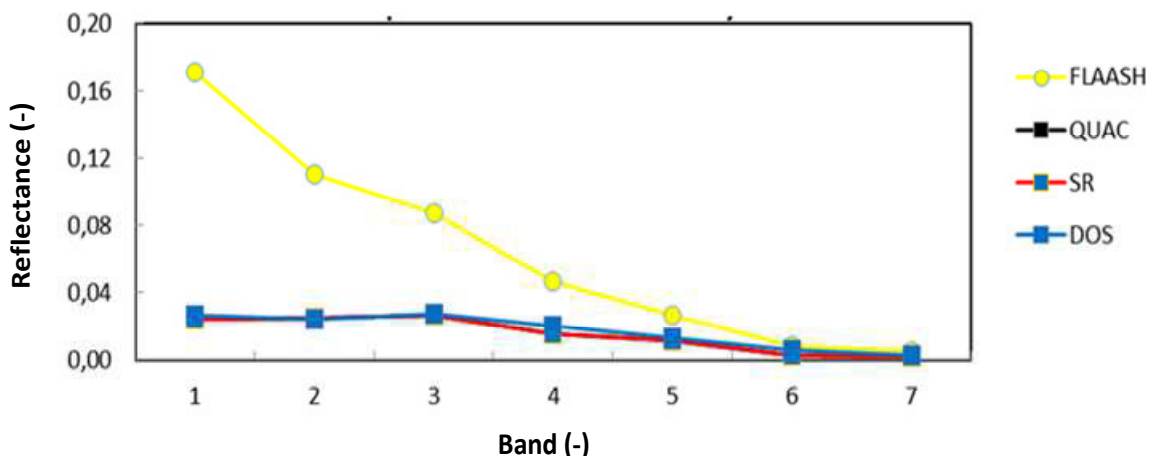
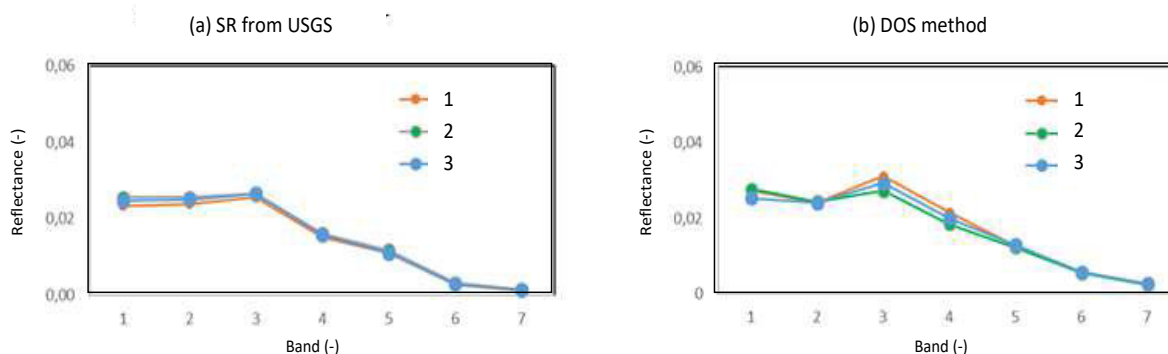Figure 3-11: Average Surface Reflectance of Water in Three Sample Locations

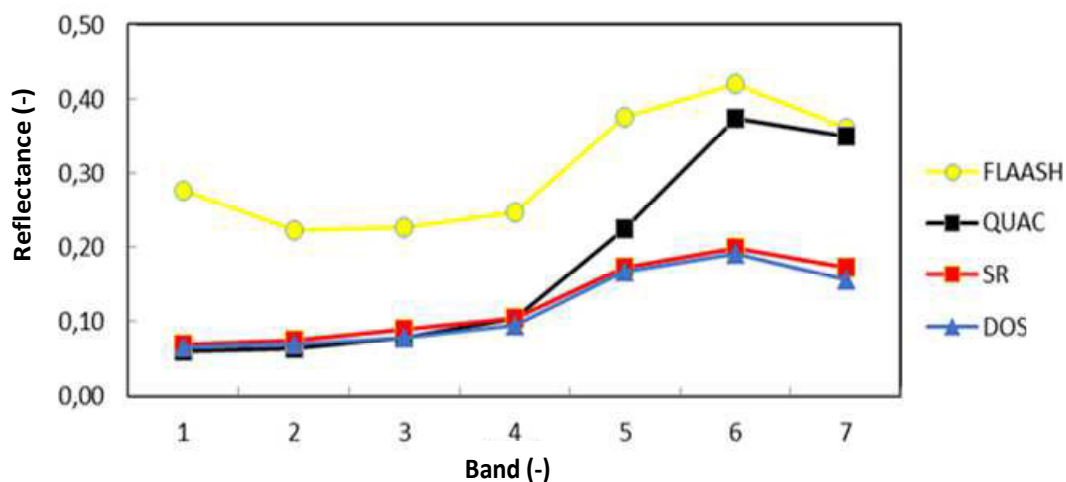Figure 3-12: Water Spectral Profile of Three Sample Locations for SR and DOS

Figure 3-13: Average Surface Reflectance of Soil in Three Sampling Locations
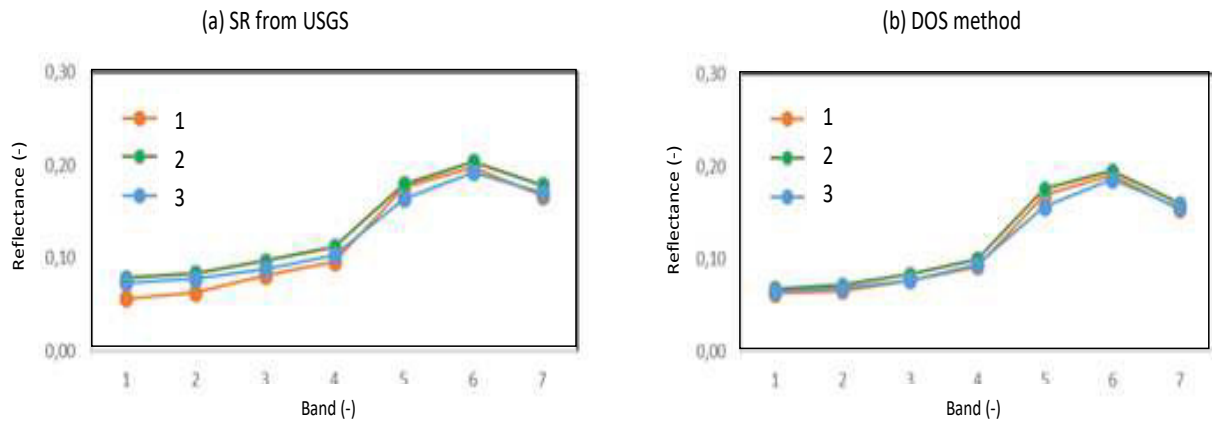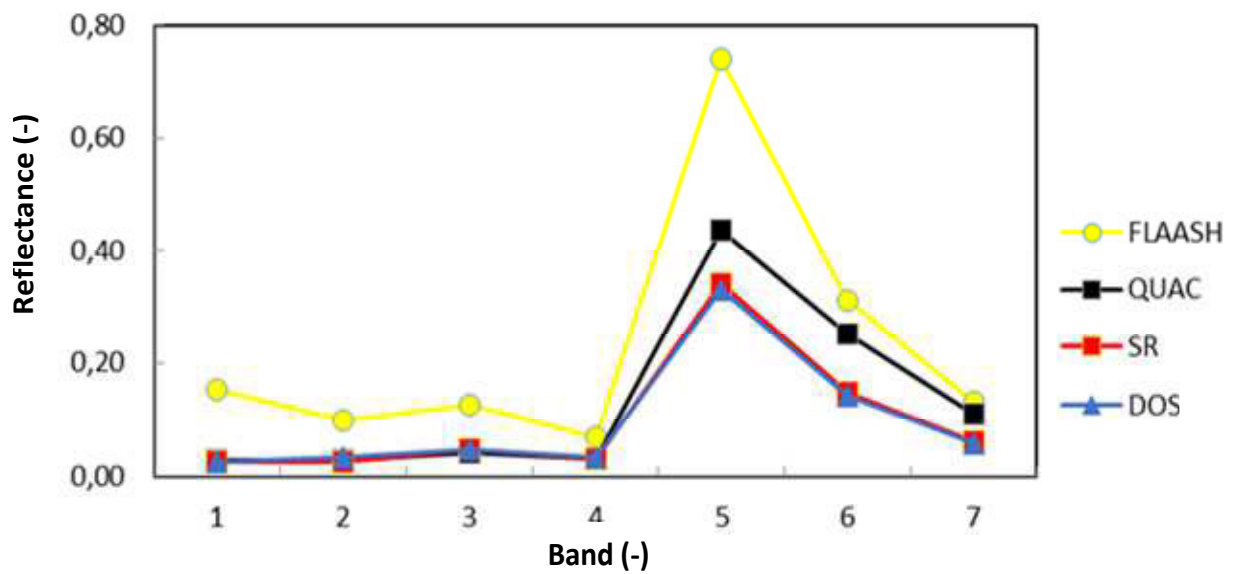
(a) SR from USGS

(b) DOS method

Figure 3-14: Soil Spectral Profile of 3 Sample Locations for SR and DOS

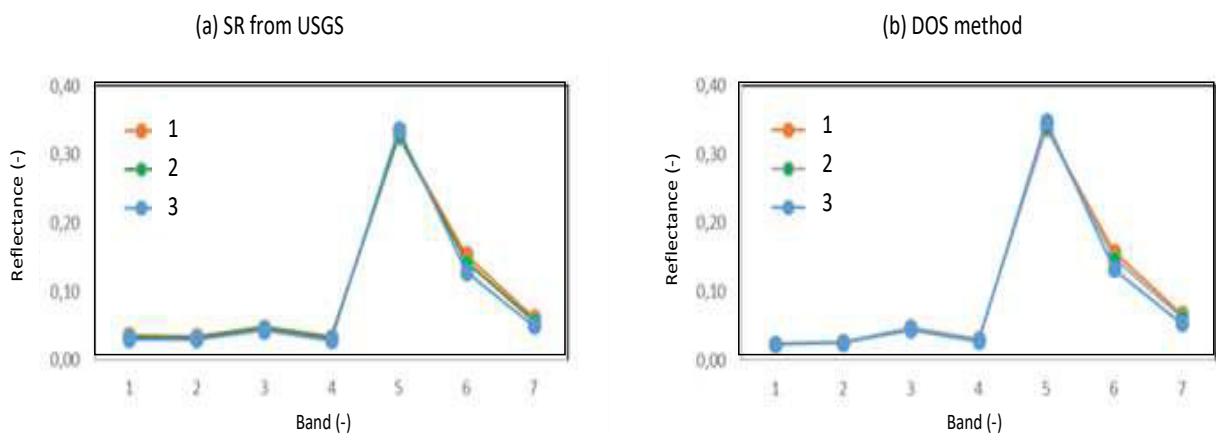Figure 3-15: Average Surface Reflectance of Vegetation in Three Sampling Locations

(a) SR from USGS

(b) DOS method

Figure 3-16: Vegetation Spectral Profile of Three Sample Locations for SR and DOS

3.2.3 Temporal spectral curve

The temporal analysis of images corrected using DOS method showed that absolute value of water, settlement (soil), and vegetation (forest) sampling were almost the same and the spectral pattern was in accordance with the spectral library, which mean that temporal sampling was consistent and the value was correct (Figure 3-17, 3-18, 3-19).
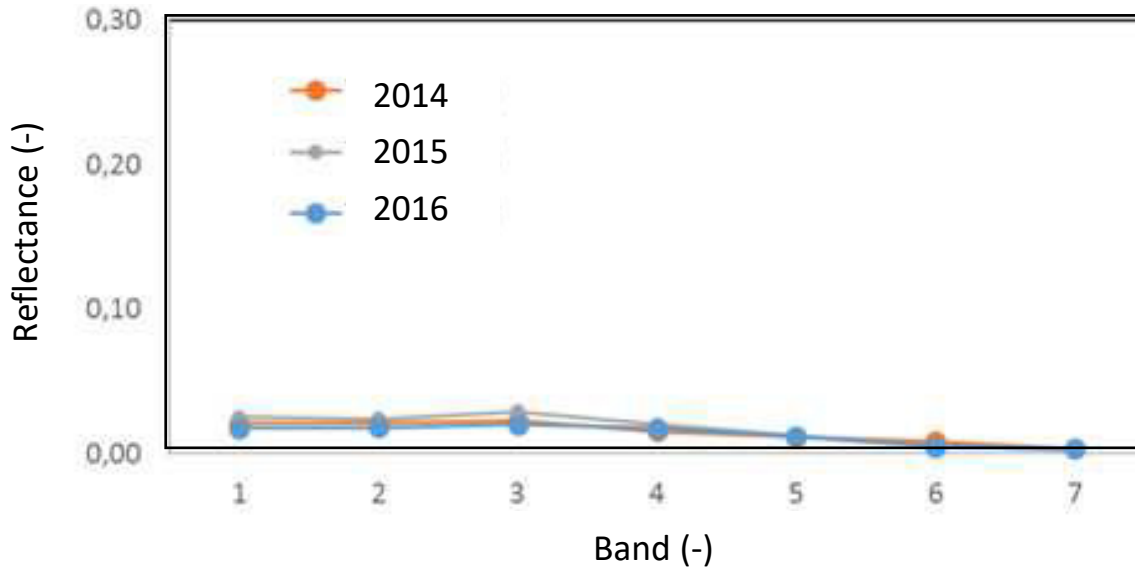

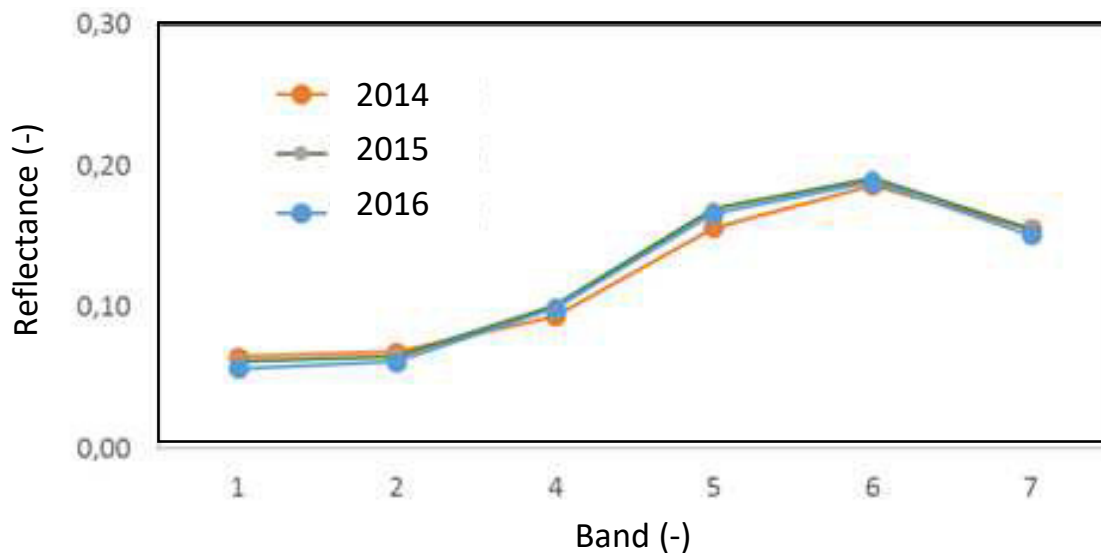Figure 3-17: Water Spectral Profiles using DOS in Different Years

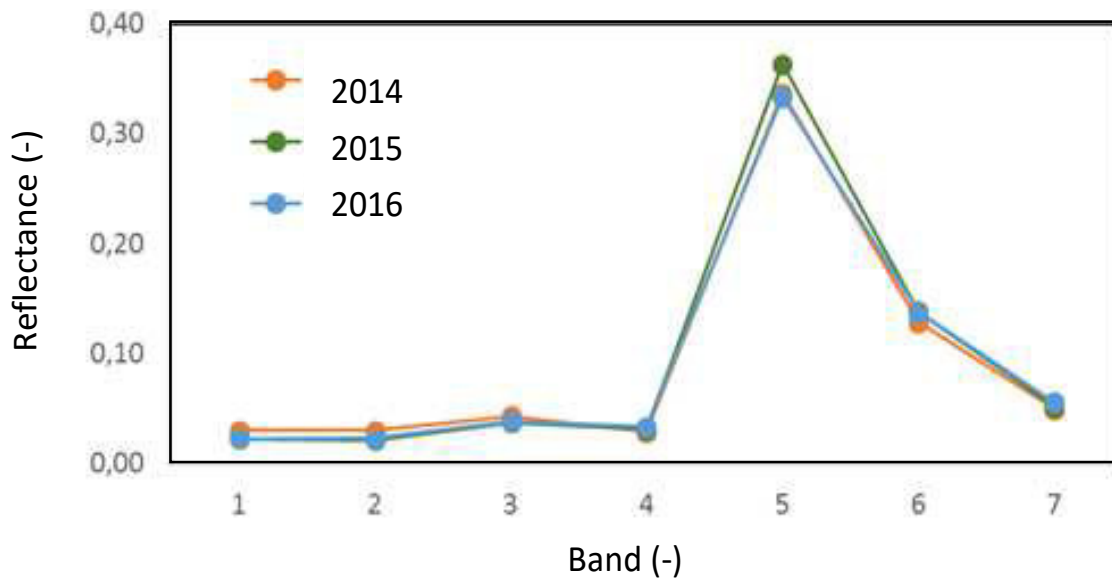Figure 3-18: Soil Spectral Profiles using DOS in Different Years

Figure 3-19: Vegetation Spectral Profiles using DOS in Different Years

4   CONCLUSION

From this analysis, it could be concluded that visual observation indicated visible contrast change on corrected image. Atmospheric correction on all models effectively reduced noise. Visually compared, FLAASH model showed the most similarity with SR image. However, the best model could not be determined by visual judgment only. It took more evaluation on spectral values. Spectral value of object corrected by DOS method was similar to USGS's SR with different absolute value of water body 0.002, soil 0.009 and vegetation 0.004, yet DOS had consistency in terms of location and region. Absolute value difference between DOS and SR was 0.001. QUAC also had similar pattern to SR, yet did not have location and time consistency. FLAASH had the highest absolute value, compared to the other models. FLAASH had location and time consistency, but when compared to SR it had significant difference on spectral pattern of visible bands, especially on blue band range.

Analysis on spectral pattern of vegetation, soil and water body showed FLAASH method was not compatible enough, although it could distinguish samples due to FLAASH and SR had great difference on the reflectance value. This was due to the type aerosol variable and atmospheric conditions of Indonesia. Both QUAC and DOS had more appropriate water body and vegetation spectral patterns. However, in terms of soil spectral pattern as compared to the average difference and deviation with SR, DOS model had more suitable object spectral pattern compared to QUAC.

REFERENCES

Caselles V., García MJL, (1989), An alternative simple approach to estimate atmospheric correction in multitemporal studies. International Journal of Remote Sensing 10(6): 1127-1134. doi: http://dx.doi.org/ 10.1080/01431168908903951.

Ceccarelli T., Smiraglia D., Bajocco S., Rinaldo S., Angelis AD, Salvati L., Perini L., (2013),

Land cover data from Landsat single-date imagery: an approach integrating pixel-based and object-based classifiers. European Journal of Remote Sensing 46 : 699 – 717.

Chavez PS, (1988), An improved dark-object subtraction technique for atmospheric scattering correction of multispectral data. Remote sensing of Environment 24 (3): 459-479. doi: http://dx.doi.org/10.1016/0034-4257(88)90019-.

Chavez PS, (1996), Image-based atmospheric corrections-revisited and improved. Photogrammetric engineering and remote sensing 62 (9): 1025-1036. Available at: http://www.unc.edu/courses/2008spring/geog/577/001/www/Chavez96-PERS.pdf/ (lastaccessed: 24/10/2016).

Cui L., Li G., Ren H., He L., Liao H., Ouyang N., Zhang Y., (2014), Assessment of atmospheric correction methods for historical Landsat TM images in the coastal zone: A case study in Jiangsu, China. European Journal of Remote Sensing 47: 701-716. doi: 10.5721/EuJRS20144740

Ginting AY, Latifah S., Rahmawaty, (2012), Analisis Perubahan Tutupan Lahan Kabupaten Karo (Analysis of Karo Regency Land Cover Changes). Peronema Forestry Science Journal 1(1).

Guo Y., Zeng F., (2012), Atmospheric Correction Comparison of Spot-5 Image Based on Model Flaash and Model Quac. International Archives of the Photogrammetry, Remote Sensing and Spatial Information Sciences, XXXIX-B7: 7-11

Lee SB, La HP, Eo YD, Pyeon MW, (2015), Generation of Simulated Image from Atmospheric Corrected Landsat TM Images. Journal of the Korean Society of Surveying Geodesy Photogrammetry and Cartography 33(1): 1-9.

Moran E., (2002), Assessment of atmospheric correction methods for Landsat TM data applicable to Amazon basin LBA research. ACT Publication No 02-06.

Nazeer M., Nichol JE, Yung Y., (2014), Evaluation of atmospheric correction models and Landsat surface reflectance product in an urban coastal environment. International Journal of Remote Sensing 35(16): 6271 – 6291. doi: 10.1080/01431161.2014. 951742.

Nguyen HC, Jung J., Lee J., Choi S., Hong S., Heo J., (2015), Optimal Atmospheric Correction for Above-Ground Forest Biomass Estimation with the ETM+ Remote Sensor. Sensors 15(8): 18865–18886. doi: 10.3390/s150818865.

Rahayu, Candra DS, (2014), Koreksi Radiometrik Citra Landsat-8 Kanal Multispektral Menggunakan Top of Atmosphere (Toa) untuk Mendukung Klasifikasi Penutup Lahan. Seminar Nasional Penginderaan Jauh.

Smith GM, Milton EJ, (1999), The use of the empirical line method to calibrate remotely sensed data to reflectance. International Journal of Remote Sensing 20 (13): 2653-2662,doi: http://dx.doi.org/10.1080/0143 11699211994.

Somdatta C., Chakrabarti S., (2011), Pre-processing of Hyperspectral Data: A case study of Henry and Lothian Islands in Sunderban Region, West Bengal, India. International Journal of Geomatics And Geosciences 2(2).

Tampubolon T., Jeddah Y., (2015), Aplikasi Pemanfaatan Citra Satelit Landsat untuk Mengidentifikasi Perubahan Lahan Kritis di Kota Medan danSekitarnya. Spektra: Jurnal Fisika dan Aplikasinya 16(2): 15-19.

Trisakti B., Suwarnana N., Cahyono JS, (2014), Pemanfaatan Data Penginderan Jauh untuk Memantau Parameter Status Ekosistem Perairan Danau (Studi Kasus: Danau Rawa Pening). Seminar Nasional Penginderaan Jauh.

Tuni MS, Barus B., Iskandar, (2013), Prediksi Perubahan Tutupan Lahan dan Perencanaan Penggunaan Lahan Pascatambang Nikel di Kabupaten Halmahera Timur. Globe 15(2): 146 – 152.

Vincent RK, (1972), An ERTS multispectral scanner experiment for mapping iron compounds. Proceedings of the Eighth International Symposium on Remote Sensing of Environment, Ann Arbor, Michigan, II: 1239-1247. Available at: http://ntrs.nasa.gov/archive/nasa/casi.ntrs.nasa.gov/19730001633.pdf/(last accessed: 24/09/2014).

Yulius, Tanto TA, Ramdhan M., Putra A., Salim HL, (2014), Perubahan Tutupan Lahan di Pesisir Bungus Teluk Kabung, Sumatra Barat Tahun 2003-2013 Menggunakan Sistem Informasi Geografis. Jurnal Ilmu dan Teknologi KelautanTropis, 6 (2): 311-318.

Zhang X., Yang H., Shuai T., (2010). Comparision of FLAASH versus Empirical Line Approach for Atmospheric Correction of OMIS-II Imagery. Journal Chinese Academy of Sciences, Beijing.

Zhang Z., He G., Wang X., (2010), A practical DOS model-based atmospheric correction algorithm. International Journal of Remote Sensing 31(11): 2837-2852, doi: http://dx.doi.org/10.1080/01431160903124682.